Intelligent PPG-based Heart Rate Signal Analysis for Car Drivers Monitoring

João Pedro Baiense[1][0009−0008−3154−7937], Anniek Eerdekens[2][0000−0001−9544−4904], Jorn Schampheleer[2][0009−0004−7194−6298], Margot Deryuck[2][0000−0002−0816−6465], Ivan Miguel Pires[3][0000−0002−3394−6762], and Fernando J. Velez[1][0000−0001−9680−123X]

[1] Instituto de Telecomunicações, DEM, Universidade da Beira Interior, 6200-001 Covilhã, Portugal
[2] WAVES, Department of Information Technology, Ghent University – imec, Technologiepark-Zwijnaarde 126, B-9052 Ghent, Belgium
[3] Instituto de Telecomunicações, Escola Superior de Tecnologia e Gestão de Águeda, Universidade de Aveiro, Águeda, Portugal

Abstract. This research aims to contribute to enhancing road safety through the development and exploration of an intelligent wristband-based health monitoring solution for car drivers. It focuses on using various sensors, such as the photoplethysmogram (PPG) and an accelerometer, to accurately estimate the drivers' heart rate. The primary goal was to create a robust and accurate model capable of real-time heart rate estimation from PPG signals, with the potential to improve the effectiveness of Internet of Medical Things (IoMT) applications in the healthcare sector. The study delves into the multiple processing steps involved in improving the quality of data to make it suitable for efficient processing by the deep learning model, encompassing data analysis, signal interpretation, and applying diverse techniques such as filters, data shifting, and data manipulation. The research integrated the leave-one-session-out (LOSO) cross-validation technique for model training and evaluation alongside fine-tuning hyperparameters to optimize model performance and efficiency. The achieved Mean Absolute Error (MAE) of 3.450 ± 1.324 bpm and Mean Squared Error (MSE) of 69.50 ± 93.57 bpm^2 represent notable outcomes, resulting in a 54.9% improvement in MAE from the original study. Additionally, the research integrated the model into a user-friendly mobile application, visually presenting the results and enabling users to examine their health status in real-time. These findings highlight the significance of meticulous data analysis and processing in wearable device applications and the high accuracy of the proposed model.

Keywords: Artificial Intelligence · Convolutional Neural Networks · Data cleaning · Data processing · Driver monitoring · Photoplethysmogram · Accelerometer · Healthcare monitoring · Heart rate signal processing · Wearable devices.

1 Introduction

The precise estimation of physiological signals from wearable devices has garnered increasing significance in recent years owing to the rising need for non-invasive and continuous health monitoring [1]. Photoplethysmography (PPG) and accelerometer data are two prevalent types of signals utilized in wearable devices to monitor various physiological parameters such as heart rate and physical activity [2].

In the domain of driver health monitoring, accurate estimation of physiological signals is imperative to ensure the safety and well-being of drivers on the road [3]. Wearable devices, including those leveraging PPG and accelerometer data, offer valuable insights into a driver's physical and physiological state [2]. For example, monitoring heart rate and physical activity can aid in identifying signs of fatigue, stress, or other health issues that may impact a driver's ability to drive a vehicle safely [4].

Nevertheless, the quality and accuracy of these signals can be significantly affected by various factors such as noise, artifacts, and device synchronization issues. Noise may emanate from diverse sources, including environmental factors like ambient light or motion, while artifacts can be attributed to device malfunctions or improper usage. Device synchronization issues may arise when the sampling rates of different sensors or devices are not properly aligned, resulting in inconsistent data [5].

To tackle these challenges, it is crucial to develop accurate deep learning (DL) models capable of effectively estimating physiological signals from wearable devices. This is particularly critical for driver health monitoring, where precise and reliable data is vital for ensuring the safety of drivers and other road users. The proposed model architecture makes a notable contribution to this field by showcasing the efficacy of deep learning models in refining health data acquired from PPG and accelerometer sensors, leading to more accurate heart rate estimations. The model is integrated into the Driver Health Tracker, an Internet of Medical Things application capable of monitoring drivers' health data via a wearable device while they are driving, and providing real-time data to the end user. This model improves the accuracy of the collected data and enhances the medical status analysis of the drivers.

The remaining of the paper is organized as follows. In Section 2, the proposed DL model is presented by describing the underlying workflow diagram while presenting details on the data set and the proposed Sliding Window technique for segmentation purposed. Exploratory Data Analysis is then pursued. In Section 3, the DL model architecture is presented by addressing the developed Convolutional Neural Network (CNN) architecture, which undergoes a series of layer computations, including convolutions and flattening, ultimately resulting in fully connected neurons and then in the heart rate estimation, as a final outcome. In Section 4, resulting form the model development in TensorFlow, its performance is determined by obtaining performance metric results. The development of a user-friendly mobile application allowed for the model deployment, as explained

in Section 5. Finally the achievements of the work are discussed in Section 6, followed by the conclusions.

2 Proposed Model

A DL model designed to estimate the user's heart rate by leveraging photoplethysmography and accelerometer data is proposed. The model aims to deliver precise estimations derived from sensor data, ensuring the fidelity and accuracy of the user's health metrics. Figure 1 illustrates the workflow for heart rate data processing.

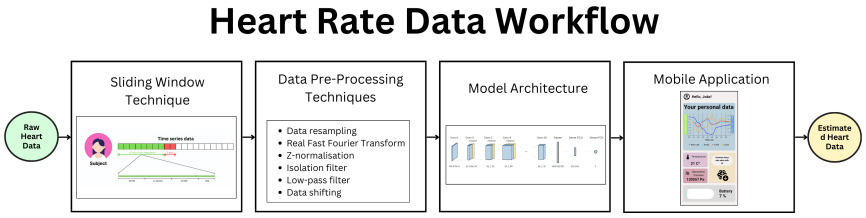

Fig. 1. Workflow diagram illustrating the heart rate data processing pipeline, from raw data input to estimated heart rate output via model algorithms and a mobile application.

Initially, raw heart rate data serves as input to the model. However, before feeding the data into the model, a Sliding Window technique [19] is applied to segment the data, followed by various pre-processing techniques. Once the data is processed, it is fed into the model algorithms to estimate the heart rate. The estimated heart rate is then displayed through a user-friendly mobile application.

2.1 Dataset

Initial training and validation of the model were conducted utilizing the PPG-DaLiA dataset [6]. The PPG-DaLiA is a publicly available dataset and provides a physiological and motion data for heart rate estimation in daily life activities. The data is recorded from both wrist- and chest-worn devices and subjects perform a wide range of activities under close to real-life conditions. The dataset was originally featured in [7] as the foundation for evaluating a CNN architecture tailored for heart rate estimation, achieving a Mean Absolute Error (MAE) metric of 7.65 ± 4.2 bpm.

The dataset is of great importance to the study's device, called Driver Health Tracker, as it contains sensor data that is highly relevant to real-life driving situations. The dataset includes PPG, accelerometer, temperature data, and records of driving activities, aligning perfectly with the objectives of the Driver

Health Tracker. By implementing the model, we have enhanced the health data captured by PPG sensors, resulting in more accurate heart rate estimates.

The dataset contains information about 15 individuals of varying ages, genders, heights, weights, skin types, and fitness levels [6]. The data was collected using two devices - RespiBAN Professional from PLUX Biosignals (worn on the chest) and Empatica E4 from Empatica [8] (worn on the wrist). Each subject followed a predefined data collection protocol comprising eight activities, including sitting, ascending and descending stairs, engaging in table soccer, cycling, driving a car, eating, walking, and working, each with an assigned time frame.

2.2 Sliding Window Technique

Following the data loading step, a preliminary analysis was conducted to evaluate the dataset's structure and content. Therefore, several data pre-processing techniques were employed to ensure its appropriateness for model development. A Sliding Window Technique was employed to facilitate analysis, which involved segmenting the sensor data into multiple windows, each having a length of 8 seconds and a shift of 2 seconds. As a result, each segment consisted of a single vector comprising 8 seconds of PPG, 3-axis accelerometer, temperature, and ECG (label) data points, as shown in Figure 2. This data segmentation method allowed for a more detailed and comprehensive sensor data analysis and its various parameters. Each 8-second segment accurately captured 512 data points for PPG, 256 data points for each accelerometer channel, 32 data points for temperature, and 1 data point for ECG, carefully considering the sampling rate of each sensor.

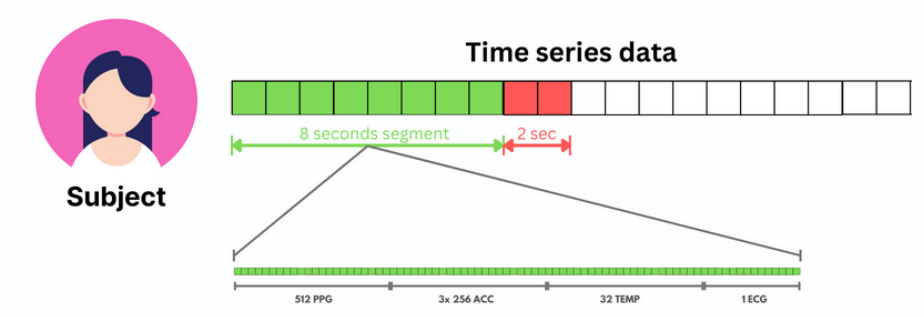

Fig. 2. Illustration of the segmentation process using a Sliding Window Technique for sensor data. Each block represents an 8-second window containing PPG, accelerometer, temperature, and ECG data points. This approach facilitates data organization and processing for subsequent analysis and model development.

2.3 Exploratory Data Analysis

The research began by analyzing the sensor data using Exploratory Data Analysis. We started by examining the PPG-DaLiA dataset. Our first goal was to carefully check the sensor readings' length, data type, and attributes. Then, we organized the dataset into 8-second segments of PPG, accelerometer, temperature, and ECG data. This method of organization allowed us to effectively visualize and scrutinize the signal properties for each subject, providing us with valuable insights into the data's characteristics. In the context of PPG-based heart rate estimation, using an 8-second sliding window with a 2-second step is a widely accepted technique, as observed in several studies (e.g., [20–24]). The 8-second window effectively captures the required information for precise heart rate estimation, while the 2-second step ensures frequent updates and aids in monitoring signal variations.

Figure 3 presents the PPG signal, which is essential for capturing changes in blood volume within the peripheral vasculature. The PPG waveform usually comprises distinct peaks and troughs corresponding to each cardiac cycle, reflecting the pulsatile nature of blood flow.

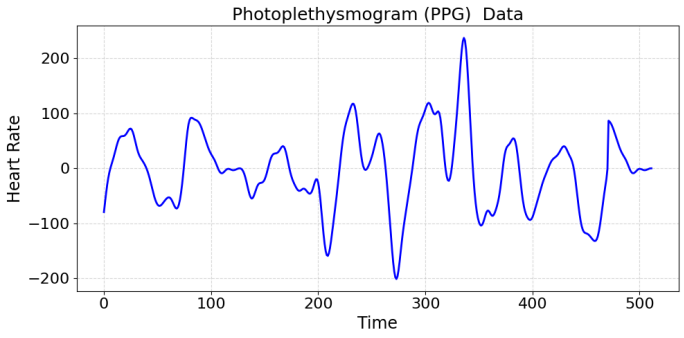

Fig. 3. Raw PPG signal of a sample segment.

Figure 4 shows the accelerometer signal, which showcases the three channels of the sensor that correspond to the motion detected from the person's wrist movements. These channels record movement along the x, y, and z axes, allowing for a thorough understanding of the direction and strength of the wrist's motion.

Finally, Figure 5 presents the accelerometer magnitude, which is a comprehensive representation of motion intensity that is obtained by combining data from the three individual accelerometer channels.

The first step of data processing was to synchronize the sampling rates of the PPG and accelerometer data. This synchronization helped align the two datasets and made it easier to analyze and interpret them cohesively. Additionally, it was observed that the accelerometer appeared to interfere with the PPG readings, resulting in a minor temporal discrepancy between the two data sets. To address

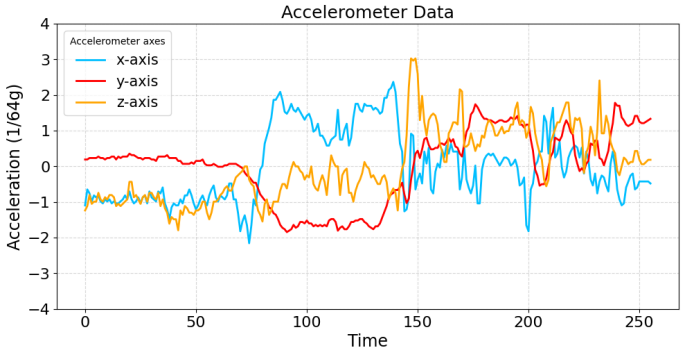

Fig. 4. Raw accelerometer signal of a sample segment.

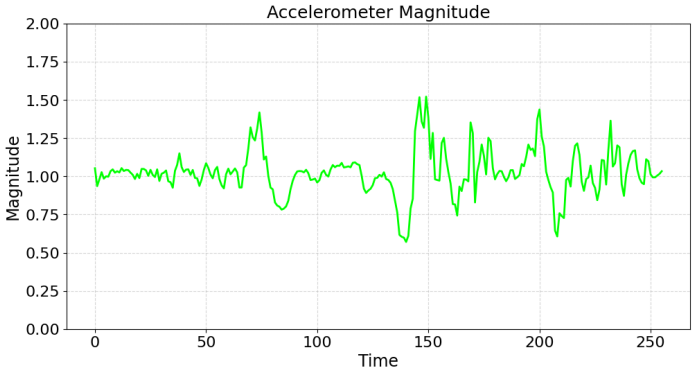

Fig. 5. Accelerometer magnitude of a sample segment.

this issue, we applied data-shifting techniques to synchronize both data sets before feeding them into the model. As a result, data synchronization between both data sets was conducted, making them suitable for further processing.

Furthermore, we identified interference from the accelerometer affecting the PPG signal. To mitigate this interference, we implemented an isolation filter to subtract the accelerometer values from the PPG data (illustrated in Figure 6). The filter incorporates a correction factor by deducting a proportionally adjusted accelerometer data from the downsampled PPG signal. The accelerometer data was first multiplied by 0.6 before being subtracted, and the resulting value was then scaled by 0.6 to account for the impact of the accelerometer on the PPG signal. The graph shows the PPG signal influenced by accelerometer signals (grey dashed line), causing distortion and noise. On the other hand, the blue solid line displays the pure PPG signal, free from accelerometer interference. This clear and reliable signal is essential for accurately analyzing cardiovascular dynamics without the impact of external factors.

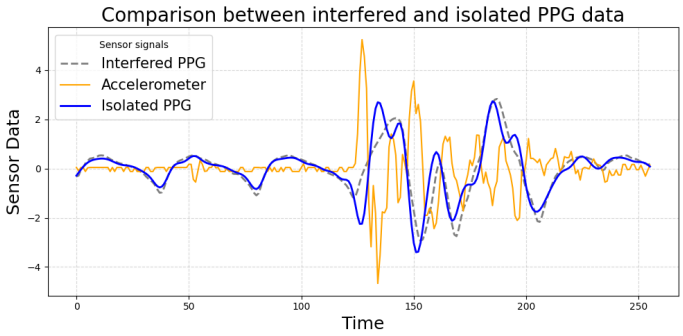

Fig. 6. Comparison of PPG signal affected by accelerometer interference and isolated PPG signal.

As a part of the data processing workflow, we applied a low-pass Butterworth filter to the PPG signal with a cutoff frequency of 4 Hz and an order of five. Figure 7 shows the difference between the unfiltered and filtered PPG signals. The unfiltered signal, although containing raw data, may display inaccuracies and noise that could obscure the underlying physiological information. On the other hand, the filtered signal yields more dependable and precise information. By efficiently removing noise and undesired frequencies, the filtered signal presents a more precise portrayal of physiological dynamics, improving the accuracy and comprehensibility of the data.

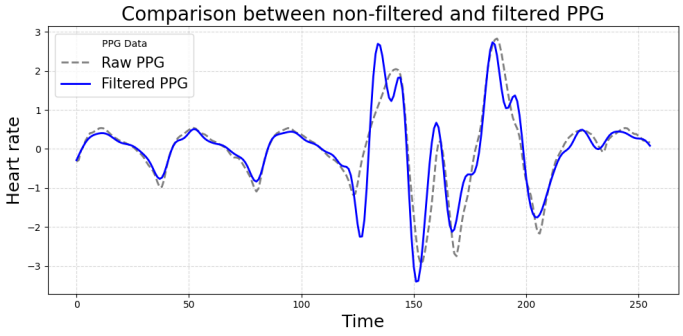

Fig. 7. Comparison between non-filtered and filtered PPG signals, highlighting the impact of filtering on signal accuracy and waveform integrity.

The Fast Fourier Transform (FFT) algorithm is commonly used in creating machine learning models. The Real Fast Fourier Transform (RFFT) is a specialized version of the FFT algorithm designed explicitly for real-number data. Using the RFFT helps us make calculations more efficient by avoiding complex numbers,

which leads to better performance. After examining the results, we found that the RFFT method produces a frequency spectrum concentrated in the 0-4 Hz range. To ensure that the data supplied to the model contains the necessary features for accurate analysis, we decided to limit the frequency range to 0-4 Hz, preserving essential information while removing unnecessary frequencies.

In order to improve the quality of the input data, the imaginary values generated by the RFFT were included in the final array, as they provide additional information about the signals. This involved performing z-normalisation on the PPG signal and the three channels of accelerometer data. This step ensures that all features are consistently scaled and that the input data is appropriately prepared for efficient processing by the model, thereby enhancing the model's performance and interpretability. Figure 8 illustrates the PPG array after applying the data processing techniques.

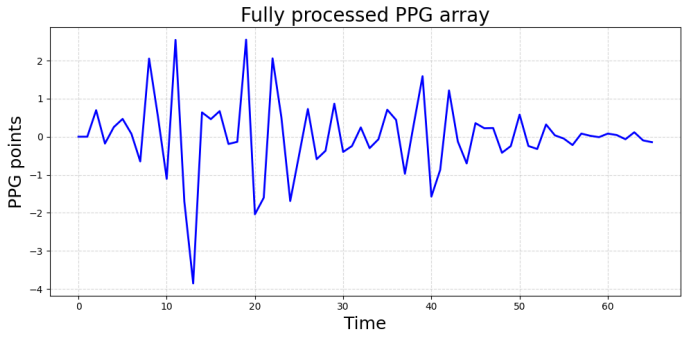

Fig. 8. Illustration of the final array after incorporating imaginary values from the RFFT and performing z-normalization on PPG and accelerometer data. These data processing techniques enhance the quality and consistency of input data for improved model performance.

3 Model Architecture

To feed the input data into our model, we organized it into a three-dimensional matrix that resembled an image structure. This matrix contained all the relevant information required for training and evaluation purposes. We developed a CNN architecture to leverage this matrix. A detailed illustration of this architecture can be found in Figure 9. The input matrix is structured as $[N_{\mathrm{RFFT}} \times N_{\mathrm{seg}} \times N_{\mathrm{ch}}]$, where N_{RFFT} represents the number of PPG and accelerometer RFFT points (66 after applying the data processing techniques), N_{seg} denotes the number of segments (standardized to 4000 segments per subject), and N_{ch} signifies the number of channels (resulting in 4 channels in total, encompassing PPG and accelerometer data). The neural network model undergoes a series of layered

computations, ultimately resulting in the heart rate estimation as the final output. The architecture of the model is presented in Figure 9.

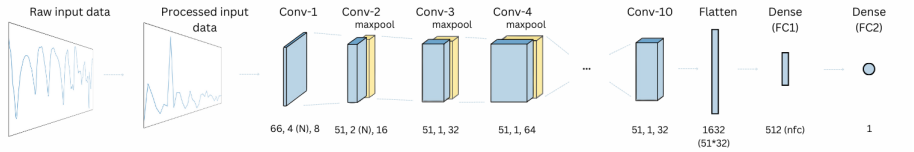

Fig. 9. Illustration of the CNN architecture developed for heart rate estimation. The input data, organized into a three-dimensional matrix resembling an image structure, contains all relevant information for training and evaluation. This CNN architecture undergoes layered computations to produce the estimated heart rate as the final output.

The Exponential Linear Unit [18] activation function is employed across the entirety of the model architecture. The final fully connected layer produces a single output: the estimated heart rate. The model is trained using a regression approach, with the metric defined as the Mean Squared Error (MSE) between predictions and the corresponding ground truth value for each segment. The MAE metric was used for evaluation, representing the average absolute difference between predictions and ground truth values. Optimization is performed using the Adam optimizer, a variant of stochastic gradient descent that adapts learning rates for each parameter.

4 Model Performance

Upon completion of the data preprocessing and generation of the input matrix, the subsequent stage entailed the development of model algorithms using TensorFlow. We utilized the leave-one-session-out cross-validation methodology during the training and evaluation phases. This helps prevent overfitting by evaluating how well the model can generalize to new data. The final model architecture comprises multiple layers totaling 2,220,577 parameters.

A series of experiments was conducted to investigate the impact of specific model settings on its overall performance. We concluded to exclude the temperature data and focus solely on the PPG and accelerometer data, as they showed the most relevance in improving the model's performance. These settings comprised the number of convolutional layers (N_L) and the dimensions of the initial fully connected layer (n^1_{fc}). Table 1 presents the outcomes of evaluating the N_L hyperparameter. In this experiment, we kept the values of n^1_{fc} as 512. The table showcases the statistical evaluation of the MAE metric for each N_L, accompanied by their respective standard deviations (referred to as STD for MAE in Table 1). Additionally, the table offers valuable information on the MSE loss function and its respective standard deviations (indicated as STD for MSE in Table 1). Upon careful analysis, it is apparent that suboptimal results are produced with

lower values of N_L when compared to higher values. Nevertheless, increasing the number of convolutional layers excessively does not necessarily guarantee improved performance. Furthermore, depending on the specific segment selected for evaluation, the model might encounter varying levels of signal clarity and noise, affecting its estimation accuracy and resulting in higher MSE standard deviations. Instead, the optimal balance is observed, and the best outcome is attained with $N_L = 6$ convolutional layers. This underscores the significance of meticulously selecting hyperparameters to achieve the optimal model performance.

Table 1. Statistical evaluation of the number of layers (N_L) hyperparameter, providing insights into the stability and performance of the model across different hyperparameter configurations.

Number of Layers (N_L)	**MAE**	**STD for MAE**	**MSE**	**STD for MSE**
1	5.407	1.792	56.44	76.53
2	5.550	1.870	59.85	83.88
3	5.560	1.980	60.53	93.37
4	5.710	2.018	63.65	104.2
5	5.484	1.905	58.74	90.87
6	5.325	1.802	54.54	85.04
7	5.434	1.732	58.74	90.87
8	5.602	2.090	61.44	105.8

In addition, further experiments were carried out to determine the ideal value for the n^1_{fc} hyperparameter. The results for various n^1_{fc} values are presented in Table 2, while N_L was kept at 6. A closer look at the data in Table 2 reveals that larger values of n^1_{fc} tend to produce better results, while smaller values lead to poorer outcomes. Specifically, the highest value tested, 1024, achieved the best results, with 512 coming in a close second with competitive results.

Table 2. Statistical evaluation of the dimensions of the initial fully connected layer (n^1_{fc}) hyperparameter, illustrating the correlation between n^1_{fc} values and model performance.

Number of fully connected layers (n^1_{fc})	**MAE**	**STD for MAE**	**MSE**	**STD for MSE**
128	7.956	1.880	56.44	76.53
256	6.469	1.804	77.46	90.88
512	5.401	1.860	60.53	93.37
1024	4.683	1.890	63.65	104.2

This finding suggests that enlarging n^1_{fc} enables the model to capture more intricate relationships within the data, resulting in improved performance. However,

it is essential to remember that while larger n_{fc}^1 values may provide slight improvements, they also come with increased computational costs. Therefore, the optimal value for this hyperparameter depends on striking a balance between performance and computational efficiency. Based on our results, we recommend using 1024 as the most optimal n_{fc}^1 value, although 512 also produces competitive outcomes.

5 Final Results

Our final model architecture development has resulted in the successful estimation of accurate and reliable heart rate values. This model is comprised of $N_L = 6$ convolutional layers and $n_{fc}^1 = 1024$ neurons in the first fully connected layer. The model's performance is evidenced by its MAE result of 3.450 ± 1.324 bpm and MSE of 69.50 ± 93.57 bpm^2. Compared to the CNN architecture in the original paper [7], our model achieves a significant 54.9% reduction in MAE. This improvement can be attributed to the implementation of advanced data processing techniques, which refine the input data, effectively reducing noise and enhancing the model's performance. The achievement marks a notable advancement in the field, showcasing the success of our model's architecture and hyperparameter tuning method. The improved performance not only enhances the accuracy and reliability of heart rate estimation but also offers valuable insights to the broader research community.

A lightweight version of the DL model has been integrated into the mobile application of the Driver Health Tracker. The application, shown in Figure 10, provides real-time access to health status, offering users deeper insight into their health condition. It serves as a central hub containing updated information and provides intuitive and accessible functionality. This proactive health monitoring approach not only enhances driver safety but also contributes to overall road safety. By promptly addressing health concerns, the application helps prevent incidents that may result from sudden medical emergencies or decreased alertness, ultimately fostering a safer driving environment for all road users.

6 Discussion and Conclusions

The accurate estimation of physiological signals is crucial in the domain of driver health monitoring to ensure the safety and well-being of drivers on the road. However, the quality and accuracy of these signals can be significantly affected by various factors such as noise, artifacts, and device synchronization issues. Addressing these challenges requires the development of accurate models capable of effectively estimating physiological signals from wearable devices. In this paper, we propose a deep learning model for estimating heart rate by leveraging photoplethysmography (PPG) and accelerometer data. The model aims to deliver precise estimations derived from sensor data, ensuring the fidelity and accuracy of the user's health metrics. Initial training and validation of the model were

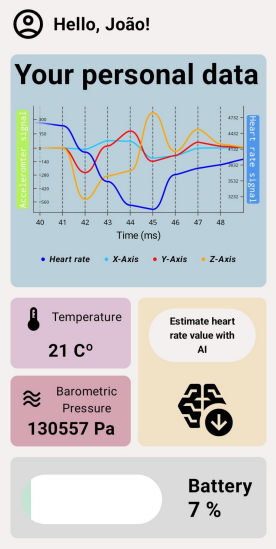

Fig. 10. Driver Health application serving as a central hub for real-time access to critical sensor data and user information.

conducted utilizing the PPG-DaLiA dataset, a renowned repository of physiological signals. Our approach involves multiple processing steps, including data analysis, signal insight, and the application of various techniques such as filters, complex algorithms, and data manipulation to enhance the quality of input data for efficient processing by the model. In conclusion, the study achieved an outstanding Mean Absolute Error (MAE) of 3.450 ± 1.324 bpm and Mean Squared Error (MSE) of 69.50 ± 93.57 bpm^2, achieving an improvement of 54.9% in MAE and demonstrating the effectiveness of the techniques employed in improving the accuracy of physiological signal estimation. Furthermore, the study successfully integrated the model into a user-friendly mobile application, allowing users to analyse their medical data in real time. These findings highlight the significance of meticulous data analysis and processing in wearable device applications and demonstrate the high performance and accuracy of the proposed model.

Furthermore, future work will focus on integrating additional features such as heart rate variability, pulse transit time, and motion artifacts to enhance data preprocessing techniques and optimize model performance. Additionally, we aim to improve the accuracy of heart rate estimation by incorporating a remote photoplethysmogram model. This model will enable heart rate measurement without direct skin contact, potentially utilizing camera-based systems.

Acknowledgements. This work was supported by FCT - Fundação para a Ciência e Tecnologia, I.P. by project reference UIDB/50008/2020, and DOI identifier https://doi.org/10.54499/UIDB/50008/2020.

References

1. Sun, W., Guo, Z., Yang, Z., Wu, Y., Lan, W., Liao, Y., Liu, Y.: A review of recent advances in vital signals monitoring of sports and health via flexible wearable sensors. Sensors **22**(20), 7784 (2022)
2. Periyasamy, V., Pramanik, M., Ghosh, P. K.: Review on heart-rate estimation from photoplethysmography and accelerometer signals during physical exercise. Journal of the Indian Institute of Science **97**, 313–324 (2017)
3. Rastgoo, M. N., Nakisa, B., Rakotonirainy, A., Chandran, V., Tjondronegoro, D.: A critical review of proactive detection of driver stress levels based on multimodal measurements. ACM Computing Surveys (CSUR) **51**(5), 1–35 (2018)
4. Antov, D., Banet, A., Barbier, C., Bellet, T., Bimpeh, Y., Boulanger, A., Zavrides, N.: European road users' risk perception and mobility: the SARTRE 4 survey. IFSTTAR (2012)
5. Böttcher, S., Vieluf, S., Bruno, E., Joseph, B., Epitashvili, N., Biondi, A., Loddenkemper, T.: Data quality evaluation in wearable monitoring. Scientific Reports **12**(1), 21412 (2022)
6. Reiss, A., Indlekofer, I., Schmidt, P.: PPG-DaLiA. UCI Machine Learning Repository, 2019, DOI: https://doi.org/10.24432/C53890
7. Reiss, A., Indlekofer, I., Schmidt, P., Van Laerhoven, K.: Deep PPG: Large-scale heart rate estimation with convolutional neural networks. Sensors **19**(14), 3079 (2019)
8. Empatica: Empatica E4 - Wearable Health Monitor, https://www.empatica.com/en-eu/research/e4/, last accessed 2024/04/09
9. Camizuli, E., Carranza, E. J.: Exploratory data analysis (EDA). The Encyclopedia of Archaeological Sciences, pp. 1–7 (2018)
10. McDuff, D., Gontarek, S., Picard, R. W.: Remote detection of photoplethysmographic systolic and diastolic peaks using a digital camera. IEEE Transactions on Biomedical Engineering **61**(12), 2948–2954 (2014)
11. Yang, C.-C., Hsu, Y.-L.: A review of accelerometry-based wearable motion detectors for physical activity monitoring. Sensors **10**(8), 7772–7788 (2010)
12. Cooley, J. W., Lewis, P. A. W., Welch, P. D.: The fast Fourier transform and its applications. IEEE Transactions on Education **12**(1), 27–34 (1969)
13. Münzner, S., Schmidt, P., Reiss, A., Hanselmann, M., Stiefelhagen, R., Dürrichen, R.: CNN-based sensor fusion techniques for multimodal human activity recognition. In: Proceedings of the 2017 ACM International Symposium on Wearable Computers, pp. 158–165 (2017)
14. Hannink, J., Kautz, T., Pasluosta, C. F., Gaßmann, K.-G., Klucken, J., Eskofier, B. M.: Sensor-based gait parameter extraction with deep convolutional neural networks. IEEE Journal of Biomedical and Health Informatics **21**(1), 85–93 (2016)
15. Hammerla, N. Y., Halloran, S., Plötz, T.: Deep, convolutional, and recurrent models for human activity recognition using wearables. arXiv preprint arXiv:1604.08880 (2016)
16. Voisin, M., Shen, Y., Aliamiri, A., Avati, A., Hannun, A., Ng, A.: Ambulatory atrial fibrillation monitoring using wearable photoplethysmography with deep learning. arXiv preprint arXiv:1811.07774 (2018)
17. Radu, V., Tong, C., Bhattacharya, S., Lane, N. D., Mascolo, C., Marina, M. K., Kawsar, F.: Multimodal deep learning for activity and context recognition. Proceedings of the ACM on Interactive, Mobile, Wearable and Ubiquitous Technologies **1**(4), 1–27 (2018)

18. Clevert, D.-A., Unterthiner, T., Hochreiter, S.: Fast and accurate deep network learning by exponential linear units (elus). arXiv preprint arXiv:1511.07289 (2015)
19. Izzeldin, H., Asirvadam, V. S., Saad, N.: Overview of data store management for sliding-window learning using MLP networks. In: 2012 4th International Conference on Intelligent and Advanced Systems (ICIAS2012), vol. 1, pp. 56–59. IEEE (2012)
20. A. Reiss, P. Schmidt, I. Indlekofer and K. V. Laerhoven. 2018. PPG-based Heart Rate Estimation with Time-Frequency Spectra: A Deep Learning Approach. UbiComp 2018 Workshop on Combining Physical and Data-Driven Knowledge in Ubiquitous Computing.
21. Z. Zhang, Z. Pi, and B. Liu. 2015. TROIKA: A General Framework for Heart Rate Monitoring using Wrist-type Photoplethysmographic Signals During Intensive Physical Exercise. IEEE Trans. Biomed. Eng. 62, 2 (2015), 522–531.
22. Z. Zhang. 2015. Photoplethysmography-based Heart Rate Monitoring in Physical Activities via Joint Sparse Spectrum Reconstruction. IEEE Trans. Biomed. Eng. 62, 8 (2015), 1902–1910.
23. T. Schaeck, M. Muma, and A. M. Zoubir. 2017. Computationally Efficient Heart Rate Estimation During Physical Exercise using Photoplethysmographic Signals. In 25th European Signal Processing Conference (EUSIPCO).
24. S. Salehizadeh, D. Dao, J. Bolkhovsky, C. Cho, Y. Mendelson, and K. Chon. 2015. A Novel Time varying Spectral Filtering Algorithm for Reconstruction of Motion Artifact Corrupted Heart Rate Signals During Intense Physical Activities using a Wearable Photoplethysmogram Sensor. Sensors 16, 1 (2015).